tion theory with β faster than the electrostatic energy. Nevertheless, it cannot by any means be precluded that the interaction is attractive. If at the same time the attraction increases rapidly with increasing coupling constant, then such a situation could be an indication of quark confinement in a less simplified model of the interaction.

The naturalness and nontriviality of the model considered here seem to me to justify publication of this paper, despite the absence of definite conclusions.

I am very grateful to V. N. Gribov for numerous stimulating discussions, which for more than two years have maintained my interest in the present problem. I am also extremely grateful to him and to A. I. Vaĭnshteĭn for a number of very important critical remarks, to L. B. Okun' for his interest in the work and valuable comments, and to B. N. Breĭzman and V. S. Synakh for a helpful discussion of the possibilities of solving the resulting equations.

1) Formally, the situation recalls the one that arises in the solution of the problem of the behavior of a small deviation of the Yang–Mills field from the Coulomb solution corresponding to a single point center.[1] However, the singularity of the vector field found in [1] in the Coulomb potential for sufficiently large coupling constant, or "the fall toward the center," is by no means peculiar to the Yang–Mills problem. This phenomenon is well known in the ordinary relativistic Coulomb problem and does not depend in renormalizable theory on the spin of the particle (in this case, the problem concerns the renormalizable interaction of a vector particle). The dependence that is found in the present paper of the solution on the magnitude of the coupling constant is peculiar to the Yang–Mills situation and certainly has no electrodynamic analog.

2) This possibility of interpreting the absence of a solution was pointed out by V. N. Gribov.

[1] J. E. Mandula, Phys. Lett. B 67, 175 (1977).

Translated by Julian B. Barbour

Intracavity laser spectroscopy with continuously and quasicontinuously operating lasers

V. M. Baev, T. P. Belikova, É. A. Sviridenkov, and A. F. Suchkov

P. N. Lebedev Physics Institute, USSR Academy of Sciences, Moscow
(Submitted 1 April 1977)
Zh. Eksp. Teor. Fiz. 74, 43–56 (January 1978)

Ways of increasing the sensitivity of the method of intracavity laser spectroscopy (ICLS) are investigated experimentally and theoretically. Factors restricting sensitivity include the selective properties of the cavity, finite time of continuous generation in the neighborhood of the line under investigation, spontaneous emission of the active medium, and spatial inhomogeneity of inversion decay in the active medium. The selective properties of the cavity can be improved by simplifying it and reducing the area of surfaces in its interior. The optimum configuration is a cavity with a single surface separating the medium under investigation from the active medium. In contrast to most other work concerned with ICLS, it is shown that the influence of spatial inhomogeneities in inversion decay is negligible in comparison with the influence of spontaneous emission in practical lasers. Spontaneous emission restricts the sensitivity of the ICLS method to $\sim 10^{-12}$ cm^{-1}. A sensitivity of 10^{-9} cm^{-1} has been achieved experimentally in the range between 0.6 and 1.06 μ. This sensitivity is determined by the time of quasicontinuous generation in the neighborhood of the absorption line under investigation. A concentration sensitivity for the detection of I_2 and NO_2 of better than 10^{-9} mole/mole has been achieved.

PACS numbers: 42.60.Da, 42.60.Kg

1. INTRODUCTION

Intracavity laser spectroscopy (ICLS)[1-20] is based on the availability of active media in which the amplification coefficient can be held constant in the neighborhood of a given absorption (amplification) line. The theoretical sensitivity limit of this method that can be attained in the case of continuous generation is determined by the ratio s_m/J_m of spontaneous to induced radiated power per longitudinal mode:

$$\delta k_l/k_{th} = s_m/J_m, \qquad (1)$$

where k_l and k_{th} are, respectively, the absorption coefficient for the given line and the threshold absorption coefficient, both averaged over the length L of the cavity.

Quantitative measurements are based on the time dependence of the generated spectrum. The time t of stable generation in the neighborhood of a given line, necessary for the intensity to fall by a factor of e, is related to $\delta k_l(\omega_0)$ and the velocity of light by the following formula:[1,9]

$$t = 1/c\delta k_l(\omega_0) \quad (\delta k_l \gg k_{th}\, s_m/J_m). \qquad (2)$$

In lasers with an inhomogeneously broadened amplification band, the amplification coefficient can be held constant with a high degree of precision due to inhomogeneous saturation in a spectral interval comparable with the amplification band width. For example, in

 0038-5646/78/4701-0021$02.40

neodymium glass lasers, one can readily achieve a generation band width of 100 cm^{-1} for an amplification band width of 200 cm^{-1}.[5] A total of 10^4 modes are then simultaneously generated. With this number of generated modes, the decay of the inverted population $n(x)$ along the generation axis occurs relatively uniformly and need not be taken into account. Under the conditions of free generation, dyes exhibit homogeneous broadening,[17] but the amplification linewidth itself is very large ($\Gamma \sim 100$ cm^{-1}). At the center of the amplification line, the amplification coefficient $k(\omega)$ can be written in the form

$$k(\omega-\omega_0)=k(\omega_0)[1-(\Delta\omega/\Gamma)^2], \quad \Delta\omega=\omega-\omega_0.$$

The width γ of the lines under investigation, for example, under atmospheric conditions, is usually ~0.05 –0.2 cm^{-1}. It is sufficient to have a generated spectrum width $\Delta\omega \sim 1$ cm^{-1} to detect this by the ICLS method. It is clear from the results reported by Suchkov[1] that the relative change in the amplification coefficient $k(\omega)$ within the interval $\Delta\omega$ for $\Delta\omega \sim 1$ cm^{-1} and $\Gamma \sim 1000$ cm^{-1} is $\sim 10^{-6}$. For $k_{th}(\omega_0) \sim 10^{-4}$ cm^{-1}, the absolute departure from constancy of the amplification coefficient in the interval $\Delta\omega$ is $\sim 10^{-10}$ cm^{-1} and this is, in principle, sufficient for the detection of a line with an absorption coefficient $k_l \geq 10^{-10}$ cm^{-1}.

However, for given cavity length in the dye laser, the number of generated longitudinal modes for $\Delta\omega \sim 1$ cm^{-1} is reduced by a factor of 100 as compared with the neodymium glass laser. Moreover, this is accompanied by a sharp increase in longitudinal inversion decay inhomogeneities and in their influence on the generation spectrum. Changes in the generation spectrum due to decay inhomogeneities may turn out to be so substantial that the line under investigation becomes undetectable against the background due to these inhomogeneities. Longitudinal inhomogeneities can, in fact, be avoided, for example, by producing unidirectional generation in a ring cavity. At the same time, the high sensitivity of the method to selective losses in the cavity means that "parasitic selection" due to, for example, interference effects, must be prevented, so that its influence on the generation spectrum is substantially smaller than the influence of the line under investigation. In a straight cavity, the level of parasitic selection is lower because of the smaller number of elements and, therefore, studies of the ICLS method under the conditions of inhomogeneous decay of the active medium at the nodes and antinodes of standing waves in the straight cavity are of undoubted interest. Theoretical studies of this problem were begun by Hansch *et al.*[16] and were continued by Stepanov *et al.*[17] They were carried out within the framework of the rate equations, including spatial effects, and were used by Statz and de Mars[21] to explain multimode generation.

Unfortunately, the analysis and conclusions reported by Hansch *et al.*[16] and Stepanov *et al.*[17] were based on the assumption that the active medium filled the cavity volume uniformly. Estimates of the limiting sensitivity based on this assumption yield values of 10^{-5}–10^{-7} cm^{-1}. We have obtained a sensitivity of the order of 10^{-8}–10^{-9} cm^{-1} and have shown that this sensitivity is restricted only by the actual time of generation in the neighborhood of the line under investigation and not by spatial inhomogeneities. This is so because the length of the active region is usually a small part of the total length L of the cavity. For example, in continuously operating dye lasers, the thickness l of the active region formed by the freely flowing stream of the dye solution is 0.1–1 mm, whereas the length of the cavity is $L \sim 1000$ mm. Hansch *et al.*[16] gave the small magnitude of l as the reason for the fivefold excess of their measured sensitivity of the ICLS method ($\sim 10^{-5}$ cm^{-1}) as compared with the value predicted on the basis of the mathematical model of the dye laser in which it is assumed that the active medium fills the entire cavity uniformly. We note that no attempt was made by Hansch *et al.*[16] to increase the sensitivity of the ICLS method by minimizing selection (for example, the cavity used by these workers contained two mirrors on plane-parallel substrates). Antonov *et al.*[14] increased the sensitivity of the ICLS method in the case of continuously-operating lasers to 10^{-7} cm^{-1} and, in their work, the sensitivity was restricted by the true time of continuous generation, which did not exceed 400 μsec.

In this paper, we report a theoretical and experimental study by the ICLS method of the generation spectrum of the continuously-operating dye laser. In accordance with the foregoing, most of the attention is devoted to longitudinal inhomogeneities in inversion decay, bearing in mind the fact that the thickness l of the active region is a small fraction of the total length L of the cavity. The position $x_0 (0 \leq x_0 \leq L)$ of the active medium relative to the mirrors, the angle φ of the plane of the stream to the axis of the cavity, and spontaneous emission are also taken into account.

2. THEORETICAL ANALYSIS OF THE GENERATION SPECTRUM

When the active medium occupies only part of the cavity length, effects connected with inhomogeneities in the active medium are accompanied by effects connected with the boundaries of the active region (boundary effects).[22] For example, in the limiting case of an infinitesimally thin active region located at the point x_0 and oriented at right-angles to the optical axis ($\varphi = 0$), the amplification is a maximum for modes that have a node at x_0, and is zero for modes that have an antinode at x_0. As the length of the active medium increases, the difference between the maximum and minimum amplification is reduced in proportion to $\lambda/2l$, where λ is the wavelength of the radiation. There is an analogous reduction in this difference with increasing φ. In contrast to volume effects, the influence of the boundary effects does not depend on the number of modes. Moreover, the influence of the relative disposition of the boundaries of the active regions between the nodes and antinodes of a mode m' on its amplification $k_{m'}$ is appreciable even for a very small excess of the pump above the threshold, i.e., even in the absence of volume inhomogeneities in the inversion population: $n(x) \equiv n_0$. To determine $k_{m'}$ it is then necessary to integrate

$k_{m'}(r) \propto n_0 E_m^2(r)$ over the volume V of the active medium. We shall assume that the continuously-operating dye laser generates the single transverse mode with a Gaussian caustic $E^2(r) \propto \exp\{-(z^2+y^2)/R^2\}$, where y, z are coordinates in the plane perpendicular to the axis of the cavity (the x axis). We have

$$\int_V E^2(r)\,dV = \int_{-\infty}^{+\infty}\int_{-\infty}^{+\infty}\int_{X_-}^{X_+} \exp\left(-\frac{z^2+y^2}{R^2}\right)\sin^2\frac{\pi m' x}{L}\,dx\,dy\,dz$$

$$= \frac{\pi l R^2}{2}\left[1 - \frac{L}{\pi l m'}\sin\frac{2\pi m' l}{L}\cos\frac{2\pi m' x_0}{L}\exp\left\{-\left(\frac{2\pi R\,\mathrm{tg}\,\varphi}{\lambda}\right)^2\right\}\right], \qquad (3)$$

where $X_\pm = x_0 \pm l/2 + y\tan\varphi$.

The second term in the brackets describes the relative effect of the boundaries of the active region on amplification:

$$k_{m'} \infty N_0 \int_V E_{m'}^2(r)\,dV.$$

In (3), R is the radius of the caustic and λ is the wavelength of the radiation. It is clear from (3) that the influence of the boundaries falls in proportion to $L/\pi l m' = \lambda/2\pi l$ as the thickness l of the stream increases. Their influence decreases still faster as $|\varphi|$ increases. If we suppose that, for $m' = 2\times10^6$, $l = 0.5$ mm, and $L \sim 10^3$ mm, which are typical values for continuously-operating dye lasers, we find from (3) that

$$\int_V E_{m'}^2(r)\,dV \approx \frac{\pi l R^2}{2}\left[1 \pm 3\cdot10^{-4}\exp\{-(120\,\mathrm{tg}\,\varphi)^2\}\right]. \qquad (4)$$

It is clear from this result that, when $\tan\varphi \leqslant 0.01$, the influence of boundary effects on the amplification $k_{m'}$ is substantial and may prevent the detection of weak lines. However, the usual procedure for reducing losses is to rotate the plane of the stream of the dye solution through an angle φ close to the Brewster angle, and $\tan\varphi \sim 1$. Equation (4) shows that the influence of the boundaries of the active region on the amplification $k_{m'}$ is then negligible. Accordingly, when we take longitudinal spatial inhomogeneities into account, we shall not henceforth complicate the equations by including the transverse structure of the field or the boundary effects.

The initial balance equations for the analysis of the generation spectrum, which take into account nonuniform decay of inversion at the nodes and antinodes of standing waves in the cavity, assuming an empty lower level, can be written in the form

$$\frac{dn(x,t)}{dt} = \rho - \frac{n(x,t)}{\tau} - n(x,t)\sum M_{m'}\frac{B_{m'}}{L}\sin^2\frac{\pi m' x}{L}, \qquad (5)$$

$$\frac{dM_{m'}}{dt} = -\frac{M_{m'}}{T_{m'}} + B_{m'}(M_{m'}+1)\int_{x_0-l/2}^{x_0+l/2}\frac{n(x,t)}{L}\sin^2\frac{\pi m' x}{L}\,dx, \qquad (6)$$

where $n(x,t)$ is the population of the upper level, M_m is the number of photons corresponding to the m-th mode, ρ is the pump, τ is the lifetime of the active particles in the upper level, and $T_{m'}$ and $B_{m'}$ are, respectively, the photon lifetime in the cavity and the probability of stimulated emission at the frequency $\omega_{m'}$. The equation for the number of photons includes a factor representing spontaneous emission:

$$dM_{m'}/dt \propto B_{m'}(M_{m'}+1)$$

where it is assumed that the two polarizations are equally probably.

Longitudinal inhomogeneities and spontaneous emission determine the distribution of the radiation over the spectrum of $M_{m'}$, but have very little effect on the total number of photons in the cavity, $I_0 = \Sigma M_{m'}$, or the mean density n_0 of active particles. The population $n(x,t)$ can, therefore, be written in the form

$$n(x,t) = n_0 + n_1(x,t) \quad (n_1(x,t) \ll n_0). \qquad (7)$$

For $M_{m'}$ we have the following additional condition

$$\sum M_{m'} = I_0. \qquad (8)$$

The quantities n_0 and I_0 in (7) and (8) are the stationary solutions of the simplest set of rate equations

$$\frac{dn(x,t)}{dt} = \rho - \frac{n}{\tau} - B_0 n\frac{I}{L}, \quad \frac{dI}{dt} = -\frac{I}{T_0} + B_0 n\frac{I}{L}. \qquad (9)$$

Substituting (7) in (5), and recalling that $n_1(x,t) \ll n_0$, we have

$$n(x,t) = n_0 + \frac{n_0^2}{\rho}\sum\frac{M_{m'}B_{m'}}{L}\cos\frac{2\pi m' x}{L}. \qquad (10)$$

If we now substitute this equation into (6) and, for simplicity, integrate for $x_0 = L/2$ (longitudinal inhomogeneities are minimal at the center of the cavity) but neglect boundary effects in accordance with (4), we obtain the following expression for the mode q':

$$\frac{dM_{q'}}{dt} = -\frac{M_{q'}}{T_{q'}} + (M_{q'}+1)\left[\frac{B_{q'}n_0 l}{L} - \frac{B_{q'}n_0^2}{\rho L^2}\sum_{m'}(-1)^{m'-q'}M_{m'}B_{m'}\frac{\sin[\pi(m'-q')l/L]}{2\pi(m'-q')/L}\right]; \qquad (11)$$

where, for $m' = q'$,

$$\frac{\sin[\pi(m'-q')l/L]}{2\pi(m'-q')/L} = \frac{l}{2}.$$

Expanding $\sin[\pi(m'-q')l/L]$ in (11) into a series up to the term $(l/L)^3$ inclusive (we recall that, in practise, $l/L \sim 10^{-3}-10^{-4}$), we obtain

$$\frac{dM_q}{dt} = -\frac{M_q}{T_q} + \frac{M_q B_q n_0 l}{L} + \frac{B_0 n_0 l}{L}$$

$$-M_q(-1)^q\frac{B_0^2 l n_0^2}{2\rho L^2}\left[C - \frac{\pi^2 l^2}{6L^2}(E - 2qD + q^2 C)\right], \qquad (12)$$

where $q = q' - m_0$, $m = m' - m_0$, so that ω_{m_0} corresponds to the maximum of the amplification coefficient $k(\omega_m)$, and

$$C = \sum_m(-1)^m M_m, \quad D = \sum_m(-1)^m m M_m, \quad E = \sum_m(-1)^m m^2 M_m. \qquad (13)$$

The first two terms on the right-hand side of (12) describe, respectively, the losses and amplification of radiation in the cavity, whereas the first term is independent of M_q and determines the contribution of spontaneous radiation. The last term describes the influence of longitudinal inhomogeneities in $n_1(x,t)$ on the generation spectrum. This term is absent in the case of unidirectional generation in a ring laser. Let us begin with this case.

Neglecting the last term in (12), we have, for stationary conditions ($dM_q/dt=0$),

$$M_q=\left(\frac{L}{T_q B_q n_0 l}-1\right)^{-1}. \tag{14}$$

The quantity $\beta(\omega_q)=L/T_q B_q n_0 l$ is the ratio of losses to amplification of radiation:

$$\beta(\omega_q)=k_{\text{пот}}(\omega_q)/k_{\text{ус}}(\omega_q). \tag{15}$$

Since (6) includes a contribution of spontaneous emission to M_q, the function $\beta(\omega_q)$ is somewhat greater than unity. The lack of amplification as compared with losses (say, per one pass) is compensated by photons emitted spontaneously during this time, and this also ensures that the stationary conditions are maintained. Near the maximum of the generation band, and in the absence of absorption lines within the cavity, we may write

$$\beta(\omega_q)=\beta(\omega_0)\left[1+\left(\frac{2q\delta\omega}{\Gamma'}\right)^2\right], \tag{16}$$

where ω_0 corresponds to the center of the amplification band, $\delta\omega=\pi c/L$ is the frequency difference between neighboring modes, and Γ' is the width of the amplification band, including a contribution due to the broad-band cavity selection used to tune the generation frequency. Substituting (16) in (14), and using (8), we find that the generation spectrum has the dispersion profile with width at half-height given by $\gamma=\delta m\delta\omega$. For δm we then have

$$\delta m=\frac{\pi}{2}\left(\frac{\Gamma'}{\delta\omega}\right)\frac{1}{I_0}. \tag{17}$$

The relative reduction in amplification due to spontaneous emission (as compared with losses at the frequency ω_0) is determined by the expression

$$\beta_0-1=\frac{\pi^2}{4}\left(\frac{\Gamma'}{\delta\omega}\right)\frac{1}{I_0^2}=\frac{1}{M_0}. \tag{18}$$

It will be useful to consider a numerical example: suppose there is no selection in the cavity and $\Gamma'=2000$ cm^{-1}, $T_0=3\times10^{-8}$ sec; generated power, including radiation losses, $P=0.01$ W, $\lambda=5\times10^{-5}$ cm, and $L=50$ cm. In this example, the total number of photons in the cavity is given by

$$I_0=\rho T_0/\hbar\omega\approx7.5\cdot10^8,\quad \delta m=10^2,\quad \delta m\delta\omega\sim1\,\text{cm}^{-1}.$$

If there is an absorption line at the frequency ω_0 with a dispersion profile and width $\gamma_l=\Delta m\delta\omega\sim0.1$ cm^{-1}, which is typical for atomospheric pressure, and absorption coefficient $k_l(\omega_0)$, we find from (14) that the generation spectrum exhibits a valley which also has the dispersion profile with width γ_v which, for $\gamma_v\ll\gamma=\delta m\delta\omega$, is given by

$$\gamma_{\text{th}}=\gamma_l\left[1+\frac{k_l(\omega_0)}{k_{\text{th}}(\beta-1)}\right]^{1/2}. \tag{19}$$

The generated intensity at the frequency ω_0 which corresponds to the center of the absorption line is given by

$$M_l(\omega_0)=M(\omega_0)\left(1+\frac{k_l(\omega_0)}{k_{\text{th}}(\beta_0-1)}\right)^{-1}. \tag{20}$$

Equations (19) and (20) determine the change in the stationary generation spectrum when a weak absorption line is introduced into the cavity in the case where (1) the valley width $\gamma_v\ll\gamma$ is much smaller than the generation linewidth, (2) the valley is at the center of the generation line, and (3) the stationary generation spectrum is determined exclusively by spontaneous emission.

To investigate spatial inhomogeneities in the decay of active particles on the generation spectrum, we return to Eq. (12). To exhibit the influence of spatial inhomogeneities in a pure form, we ignore for the moment the term $B_0 n_0 l/L$, which is responsible for spontaneous emission. We then have

$$\frac{dM_q}{dt}=-\frac{M_q}{T_q}+\frac{M_q B_q n_0 l}{L}-M_q(-1)^q\frac{B_0^2 l n_0^2}{2\rho L_0}\left[C-\frac{\pi^2 l^2}{6L_0}(E-2qD+q^2C)\right]. \tag{21}$$

The last term in (21) represents the spatial inhomogeneity of decay and is a parabolic function of q but changes sign as $(-1)^q$.

If there are no absorption lines in the cavity, the sum of the first two terms (losses and amplification) is also a quadratic function of q. This means that the condition $dM_q/dt=0$ can be simultaneously satisfied only for three values of q. For all other values, $dM_q/dt<0$.

Thus, under steady-state conditions, there are only three modes in the interval of values of q for which $|2\pi l_q/L|<\pi/4$, and the expansion of $\sin[\pi(m-q)l/L]$ into a series is valid. We recall that we are considering the case where $l/L\sim10^{-3}-10^{-4}$ and the active region is located at the center of the cavity. When M_0 is at the center of the amplification line, $M_{+1}=M_{-1}$ (symmetric case). The solution of (21) with $M_{-1}+M_0+M_{+1}=I_0$ yields

$$M_{\pm1}=\frac{\rho lT_0}{4}\,\frac{\eta-1-\eta(2\delta\omega/\Gamma)^2}{1-\pi^2l^2/12L^2}, \tag{22}$$

$$M_0=\frac{\rho lT_0}{4}(\eta-1); \tag{23}$$

where η is the relative excess of the pump over the threshold ($\eta=\rho/\rho_{\text{th}}$).

The presence of three modes is due to the fact that spatial inhomogeneity in the decay of the active medium ensures that the reduction in amplification for side modes is compensated by an increase in the number of active particles falling into the nodes of these oscillation modes. This additional amplification is $k_{\text{th}}(2\delta\omega/\Gamma)^2\sim10^{-14}$ cm^{-1}, i.e., it is much smaller than the contribution of spontaneous emission. It may be expected that longitudinal inhomogeneities in the inverted population will have a very slight effect on the generation spectrum obtained when only spontaneous emission is taken into account.

The solution given by (22) is physically interesting only when the generation spectrum determined by spontaneous emission contains a small (~3–10) number of modes. In this case, it is necessary to investigate the combined influence of spontaneous emission and inhomogeneities in the decay of the active medium on the generation spectrum.

Suppose that the generation spectrum, which has the dispersion profile (17), contains a dispersion valley (19), (21) at its center, due to an absorption line. Let us write the spectrum in the form

$$M_q=\frac{M_0}{1+(q/\delta m)^2}-\frac{M_0-M_l}{1+(q/\Delta m)^2}. \tag{24}$$

To obtain a direct estimate of the influence of longitudinal inhomogeneities in inversion on the generation spectrum, let us evaluate the last term in (21), which is responsible for the additional amplification due to the spatial distribution of inversion:

$$\delta\frac{dM_q}{dt}=-M_q(-1)^q\frac{B_0^2n_0^2l}{2L\rho}\left[C-\frac{\pi^2l^2}{6L}(E-2qD+q^2C)\right]. \tag{25}$$

We restrict our attention to the symmetric case $M_{-q}=M_{+q}$. We have

$$D=\sum(-1)^q qM_q=0.$$

The case $\delta m \gg \Delta m \gg 1$ is important in practise and, for this case, we have

$$C=\sum(-1)^q M_q=M_0\frac{\pi\delta m}{2}\exp\left(-\frac{\pi\delta m}{2}\right)-(M_0-M_l)\frac{\pi\Delta m}{2}\exp\left(-\frac{\pi\Delta m}{2}\right), \tag{26}$$

$$E=\sum(-1)^q q^2M_q=M_0\frac{\pi(\delta m)^3}{8}\exp\left(-\frac{\pi\delta m}{2}\right)-(M_0-M_l)\frac{\pi(\Delta m)^3}{8}\exp\left(-\frac{\pi\Delta m}{2}\right). \tag{27}$$

Substituting (26) and (27) into (25), and comparing the additional amplification $\delta dM_q/dt$ with the contribution of spontaneous emission $B_0n_0l/L=1/T_0$, we obtain the following condition after some simple rearrangement:

$$M_0\frac{\Delta m}{\delta m}e^{-\pi\Delta m}\ll 1. \tag{28}$$

This ensures that the influence of spatial inhomogeneities is small. Returning now to the above special case $I_0\sim 10^8$, $\delta m\sim 10^2$, $L\sim 10^2$ cm, we see that, for spectral lines with $\gamma_l=\Delta m\delta\omega\sim 0.1$ cm^{-1} and $M_0\approx I_0/\delta m$, condition (28) is satisfied with a considerable margin.

For nonstationary generation, if we neglect the influence of spontaneous emission and the spatial inhomogeneities in inversion, we obtain the following expression from (12) for absorption lines with $k_l(\omega)\gg k_{th}(\beta-1)$:

$$M_q(t)=\frac{I(t)}{I_0}M_q(0)\exp\left\{-\left[\frac{2\delta\omega q}{\Gamma}\right]^2\frac{t}{T_0}\right\}\exp[-k_l(\omega)ct], \tag{29}$$

where the normalizing factor $I(t)$ is given by the condition $\Sigma M_q(t)=I(t)$. It is easily seen that (29) describes absorption in an optical cell with optical path length $L_{eff}=ct$.

Assuming, for simplicity, that $M_q(0)=M_0$, we see that the generation spectrum for $k_l(\omega)=0$ has a Gaussian shape of width

$$\gamma(t)=\Gamma(T_0/t)^{1/2}. \tag{30}$$

The condition for the validity of (29) is that the width $\gamma(t)$ is large in comparison with the stationary width (17) determined by spontaneous emission:

$$\Gamma\left(\frac{T_0}{t}\right)^{1/2}\gg\frac{\pi\delta\omega}{2}\left(\frac{\delta\omega}{\Gamma}\right)^2\frac{1}{I_0}. \tag{31}$$

3. EXPERIMENTAL INVESTIGATION OF THE SPECTRUM USING A DYE LASER

There are a few papers in the literature[14-16,19] in which a continuous dye laser is used in conjunction with the ICLS method. However, in all these cases, the continuous dye laser was designed so that it had minimum threshold, maximum possible efficiency, convenience of operation, and so on, but no attempt was made to satisfy the specific conditions that must be satisfied by the continuous dye laser in the case of the ICLS method. The most important of these is the absence of parasitic selection in the cavity and maximum generation stability. Attempts to reach the generation threshold led some workers to the use of three-mirror[14,15,19] or even four-mirror[16] cavities ensuring compensation of the astigmatism of the stream. In some experiments, the dye was pumped through the cell,[15,16,19] which introduced two extra elements into the cavity, namely, the cell windows. A further selecting element (for example, a prism[14]) was introduced into the cavity for wavelength tuning. However, any additional element introduced into the cavity necessarily leads to the appearance of microinhomogeneities due to, for example, any defect of this element. The presence of microinhomogeneity of size $d\leqslant\lambda/2$ and scattering cross section σ at a point x_0 in the cavity produces additional losses with period $\delta q=L/x_0$ ($x_0\leqslant L/2$, which are maximum for modes having a node at x_0, in accordance with the equation

$$\frac{dM_q}{dt}\sim-\frac{M_q}{T}-M\frac{2c\sigma\sin^2(\pi qx_0/L)}{\pi R_0^2(x_0)L}. \tag{32}$$

Let us suppose that $\sigma\sim(\lambda/10)^2$, $R_0\sim 10^{-3}$ cm (microinhomogeneity in the region of the caustic). The resulting additional losses M_q/T_σ correspond to $T=2\times 10^{-4}$ sec. Parasitic selection with period $\delta q=2$ is detected in a time T_σ.

Additional losses appear when some of the mirrors in the cavity are used at oblique incidence. Let us suppose that the direction of propagation of the radiation is at an angle α to the normal to the mirror, in which case the distribution of the radiation with this angle is

$$u(x')\sim\sin^2\frac{2\pi x'\,\mathrm{tg}\,\alpha}{\lambda}. \tag{33}$$

A mirror defect of size $d < \lambda/\tan\alpha$ will also produce parasitic selection with equivalent $\Delta kL \sim d^2/D^2$, where D is the beam diameter on the mirror. Consequently, mirror defects have the smallest influence on the spectrum when $\alpha = 0$. Moreover, additional selection is introduced by reflection from the back of the mirrors which, in some cases, are not cut at an angle to the reflecting surface, or are cut at a small angle.[14-16,19]

Adequate filtration of the dye solution and constant parameters of the active region in the working material are essential to ensure maximum generation stability. Poor filtration leads to a reduction in the true generation time (for example, to 200–400 μsec[14]) due to the complete break in generation when optical microinhomogeneities, for example, bubbles, enter the active region. These defects have meant that sensitivities better than 10^{-7} cm^{-1} have not so far been achieved by using the ICLS method with continuously-operating dye lasers.

To increase the sensitivity in accordance with the above analysis of the various factors which influence it, we have built a continuously-operating dye laser with a freely flowing stream of a solution of rhodamine 6G in ethylene glycol. The concentric cavity of the laser was formed by two mirrors with radii of curvature equal to 300 mm. The flat stream of the dye solution had a thickness of 0.2 mm and was located at the center of the resonator at the Brewster angle to the optical axis. The dye was pumped and filtered by a standard pump and a filter from a dye laser. The laser cavity mirrors had reflection coefficients of 99–99.6%, a thickness of 40 mm, and a back surface cut at 10°. The continuously-operating dye laser was pumped by a CR8 argon laser with stabilized output radiation. This radiation was focused by a lens into a 20 mm spot in the dye stream. To reduce parasitic selection in the cavity, we did not use an additional selector, and the generation-frequency tuning was achieved by varying the position of the dye stream, by rotating it, and by varying the power spectrum of the pump radiation. To avoid optical inhomogeneities (fluctuations in atmospheric density and dust), the cavity was isolated from the atmosphere by glass windows, and provision was made for flushing with an inert gas and filling with the material under investigation. The system was assembled on a vibration-free table. The continuity of generation was monitored with a photomultiplier and an oscillograph. Both radiation integrated over the entire spectrum and radiation in narrow spectral intervals containing a few modes could be monitored.

The emission spectrum was recorded with the UF-90 autocollimating camera containing a 1200-line/mm diffraction grating, 100 mm long. The grating was used in the second order. Because of the high intensity emitted by the continuously-operated dye laser, we succeeded in using threefold dispersion of the grating with the aid of a flat mirror which enabled us, at least in principle, to obtain any number of reflections from the grating and thus increase the resolution and dispersion of the spectrograph. The theoretical resolving power of the spectrograph was then 6×10^5 and the dispersion was 0.8 Å/mm. The actual resolution was etter than 0.05 cm^{-1}.

We used this system to obtain the absorption spectrum of atmospheric air in the wavelength range 585–605 nm, which was mainly due to the presence of water vapor. This spectrum was then compared with atmospheric absorption spectra obtained previously by traditional methods, using optical paths of several kilometers,[23] the ICLS method,[7,14] and tabulations of the solar spectrum.[24] Many new absorption lines, previously not seen, were discovered and lines identified

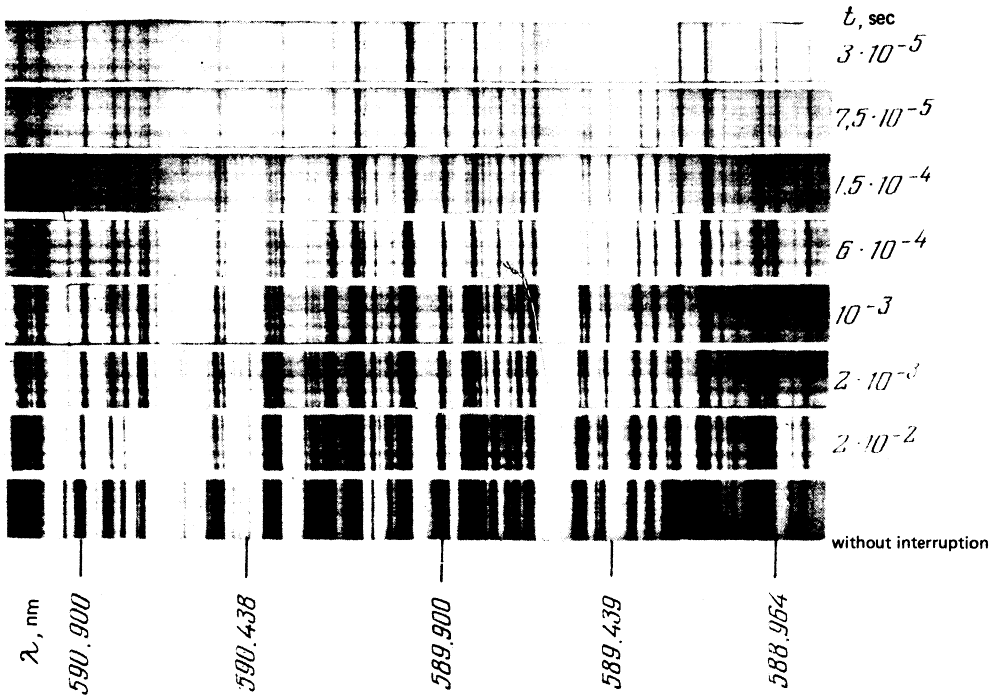

FIG. 1. Atmospheric absorption spectrum obtained with the aid of a dye laser for different generation times.

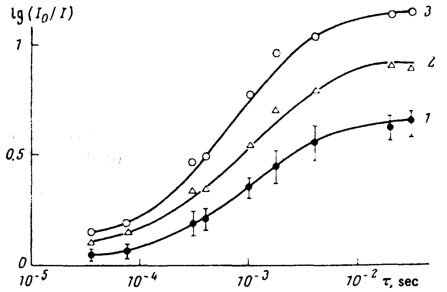

FIG. 2. Depth of valley in the dye-laser generation spectrum as a function of generation time for three different water-vapor lines with different equivalent widths [24] for the solar spectrum: 1—$\lambda = 5906, 30$ Å, $\Delta\lambda = 2 \times 10^{-3}$ Å; 2—$\lambda = 5907.48$ Å, $\Delta\lambda = 3.0 \times 10^{-3}$ Å; 3—$\lambda = 5908.21$ Å, $\Delta\lambda = 9.5 \times 10^{-3}$ Å.

erroneously as solar lines were located. Comparison of microdensitometer scans of the spectrum obtained in this way with previously published spectra shows that the sensitivity which we have attained corresponds to an optical length of the absorbing layer of not less than 1000 km. The following experiments were also carried out to determine the sensitivity of our system.

The atmospheric absorption spectrum (Fig. 1) was recorded for generation times t between 3×10^{-5} and 3×10^{-2} sec. This time was varied by mechanical chopping of the pump radiation. The effective length of the absorbing layer could thus be varied from 10 to 10 000 km. Analysis of the spectra shows the presence of a monotonic increase in sensitivity with increasing generation time, up to 0.03 sec. However, linearity was observed only up to 3msec and, for longer generation times, there were breaks in generation other than those due to modulation, and these led to deviation from linearity. This shows that the effective length of the absorbing layer was not less than 1000 km. Figure 2 shows the results obtained as a result of an analysis of these spectra. It gives the valley depth for some of the water-vapor lines[24] as a function of the generation length.

The next independent experiment was concerned with the time of stable continuous generation and was designed to determine the spectrum width when maximum stability was attained without change in the generation frequency. The width of the generation spectrum achieved in these experiments was 3 Å. The width of the amplification band of the dye was $\Gamma \sim 1000$ Å, and the relative change in the amplification coefficient in this region was $(\Delta\Gamma/\Gamma)^2 \approx 10^{-5}$. The threshold amplification coefficient was $k_{th} \sim 10^{-4}$ cm^{-1}. Consequently, the sensitivity was $\delta k \sim k_{th}(\Delta\Gamma/\Gamma)^2 \sim 10^{-9}$ cm^{-1} and corresponding time of stable generation was $t \sim 1/c\delta k \approx 3 \times 10^{-2}$ sec.

The limiting sensitivity of our system, determined by spontaneous emission, can be calculated from (1) and is $\delta k \sim 10^{-11}$ cm^{-1}, which corresponds to a generation time of 1 sec. Consequently, the sensitivity attained in our experiments is not the limiting sensitivity, but is restricted by mechanical vibrations of cavity elements, instabilities in pump radiation, and other factors producing a variation in the generation spectrum with time. The observed behavior of the generated intensity as a function of time, recorded in a narrow spectral interval of ~0.1 cm^{-1}, confirmed that the true time of continuous generation was ~0.01 sec. However, the sensitivity that we have attained is much greater than the "limiting sensitivity" calculated by Stepanov *et al.*[17] on the erroneous assumption that spatial inhomogeneity has a dominant effect on the sensitivity. This confirms the calculations given above.

To determine the concentration sensitivity of the system in the presence of iodine vapor, controlled amounts of I_2 in the range 0.001–0.1 g were introduced into the laboratory enclosure which had a volume of 200 m^3. A ventilator was used to produce uniform mixing. When 2 mg of I_2 was introduced, this could be reliably detected in the spectrum of the atmosphere. The relative concentration of I_2 under these conditions is 10^{-9} or 1 ppb. The absorption coefficient corresponding to this concentration is 10^{-8} cm^{-1}.[25]

The atmospheric spectrum was found to contain, in some intervals, both absorption and amplification lines. It was established that the intensity of the amplification lines was determined by the concentration of NO_2 in the atmosphere. As in the case of the iodine vapor, controlled amounts of NO_2 were introduced into the room by depositing known numbers of 25-mg drops of a 50% solution of nitric acid on a copper surface. The generation spectrum was then found to consist mainly of strong individual gain lines, reliably identified as being due to NO_2 (Fig. 3). These gain lines did not vanish when the concentration was reduced to the background level. The gain lines were also reported in our previous paper,[9] and an analysis of published data[26] on the spectroscopic properties of the NO_2 molecule shows that the appearance of the gain lines can be qualitatively explained by the pumping of NO_2 by the argon laser radiation.

4. EXPERIMENT WITH THE Nd^{3+} LASER

To increase the sensitivity of the ICLS method in the case of the Nd^{3+} laser,[2-4] and to investigate the dependence on time, we built a system which enabled us to vary the generation time of this laser from 5×10^{-4} to 10^{-2} sec. This was done by adding different numbers of storage capacitors (between 1 and 20, 500 μF each, coupled by suitable inductances) used to supply two pulsed ISP-250 lamps which produced inversion in the glass rod containing Nd^{3+} (diameter 4 mm, length

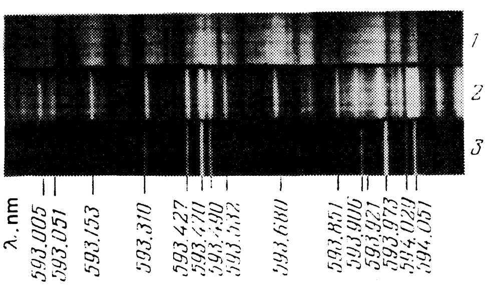

FIG. 3. Spectrum of NO_2 obtained with a continuously-operating dye laser for different NO_2 concentrations in the atmosphere: 1—10^{-8} atm; 2—2×10^{-7} atm; 3—10^{-5} atm.

50 mm). To reduce parasitic selection, the mirrors had a thickness of about 40 mm, the back face was cut at 10°, and the reflection was close to 100%. The ends of the active element were cut at the Brewster angle. The tube containing the gas under investigation was hermetically sealed at one end by a mirror and by the rod at the other end. The spectrograph was the autocollimating UF-90 tube with a 300-line/mm diffraction grating used in the fifth order with twofold dispersion. The resolving power of the spectrograph was ~0.07 cm^{-1} and the dispersion was 1.3 cm^{-1}/mm. The continuity of generation and the generation time were monitored by slit scanning and a photodiode operating in conjunction with an oscillograph. To investigate the sensitivity obtained in this way, we used CO_2 gas with different partial pressures of air up to a total pressure in the cell of 1 atm. The laser generation band contained an R branch of the ($04^03 \leftarrow 00^00$) transition (Fig. 4) for which the line intensities were known[27] [thus, for example, for the line with $j = 14$, we have $S = 0.042$ $cm^{-1}km^{-1}atm^{-1}$ ($\nu = 9399.0$ cm^{-1})].

Figure 4 shows the CO_2 absorption spectra for different generation lengths and partial pressure of CO_2 equal to 0.05 atm. In all the experiments, CO_2 was diluted with air up to 1 atm in order to broaden the lines up to 0.08 cm^{-1}. It is important to remember that the photographs show the generation spectrum corresponding to the entire pulse and, therefore, the blackening on the film is proportional to

$$\int_0^T I(t)\exp[-\alpha(\omega,t)]dt,$$

where $\alpha(\omega, t) = k(\omega)ct\Delta/L$, $\Delta l/L$ is the cavity occupation factor (in our case, 0.6), $k = pS/\Delta\nu$ is the absorption coefficient, p is the CO_2 pressure, S is the absorption line intensity, and $\Delta\nu$ is its width.

Figure 5 shows the results of an analysis of microdensitometer tracings of the above line, averaged over a large number of measurements. The graph gives the valley depth in the generation spectrum as a function of log(kct) at a number of pressures of the mixture. For generation times up to 3 msec, the graphs are identical, i.e., the reduction in pressure for the same increase in generation time produces the same valley in the spectrum. The sensitivity ceases to increase as the generation time is increased further, and this occurs more rapidly as the partial pressure of CO_2 in the cell is increased. Analysis of the slit scans of the generation spectrum shows that, as the generation time increases, the spectrum contracts, and this contraction is greater at higher CO_2 concentrations in the tube. The recorded CO_2 lines lie at the edge of the spectrum, so that the effective generation time in the region of the lines under investigation is 2.5 msec at a CO_2 pressure of 0.2 atm, and increases to 6 msec when the pressure is reduced to 0.01 atm. This is in good agreement with the results shown in Fig. 4. The contraction of the generation spectrum with increasing generation time may be connected with the fact that the amplification coefficient of the Nd^{3+} glass varies over the nonuniform spectrum, there are energy losses in the inductances in the charging system, and there is the strong integrated absorption in the R branch which produces a break in generation in this region.

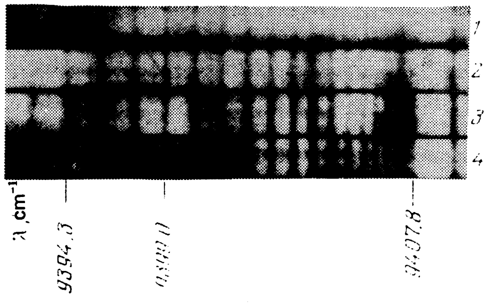

FIG. 4. Absorption spectrum of CO_2 in the atmosphere, obtained with the aid of an Nd^{3+} glass laser with different generation times: 1—5×10^{-4} sec; 2—1.3×10^{-3} sec; 3—5×10^{-3} sec; 4—10^{-2} sec. Partial pressure of CO_2 is 0.05 atm for all the spectra.

It is clear from our results that we have reliably recorded the CO_2 lines on the integrated spectrum with absorption coefficient $k = 2 \times 10^{-8}$ cm^{-1}. For water-vapor lines which are located at the generation center, this figure is 10^{-8} cm^{-1}, which corresponds to an effective length of 1000 km. This length is greater still when the scanned spectra are recorded. We have thus demonstrated that the sensitivity of the ICLS method used in conjunction with the Nd^{3+} glass laser increases as the generation time increases up to 10 msec. Restrictions due to spontaneous noise in this range have not yet been observed.

5. CONCLUSIONS

The monotonic increase in the valley depth in the generation spectra of the lasers that we have investigated up to $T = 0.01$ sec suggests that the effective length of the absorbed layer in the 0.6 and 1.06 μ bands is at present not less than 1000 km, and this does not appear to be the limiting figure because it is restricted only by the true generation time.

Our results show that the ICLS method is, in fact, the most sensitive, fast, and accessible method of detecting

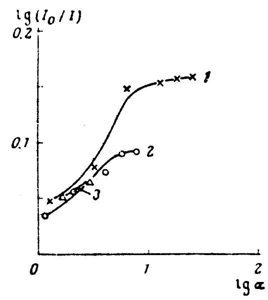

FIG. 5. Depth of valley on the CO_2 lines in the generation spectrum of the Nd^{3+} glass laser for different generation times and different CO_2 partial pressures: 1—0.05 atm, 2—0.016 atm, 3—0.006 atm. Measurements were performed for the $j = 14$ line associated with the [$04^03 \leftarrow 00^00$] vibrational transition in the R band of CO_2.

small amounts of impurities in gases but, for the purposes of certification of gas purity, it will be necessary to develop special methods because published information shows a lack of calibration techniques for the determination of impurities at the level of sensitivity and rapidity that we have attained.

[1]A. F. Suchkov, "Line structure of generation spectra due to lasers with inhomogeneously broadened gain line," Preprint No. 126, Lebedev Physics Institute, Moscow, 1970.
[2]L. A. Pakhomycheva, E. A. Sviridenkov, A. F. Suchkov, L. V. Titova, and S. S. Churilov, Pis'ma Zh. Eksp. Teor. Fiz. 12, 60 (1970) [JETP Lett. 12, 43 (1970)].
[3]T. P. Belikova, É. A. Sviridenkov, A. F. Suchkov, L. V. Titova, and S. S. Churilov, Zh. Eksp. Teor. Fiz. 62, 2060 (1972) [Sov. Phys. JETP 35, 1076 (1972)].
[4]T. P. Belikova, B. K. Dorofeev, E. A. Sviridenkov, and A. F. Suchkov, Kvantovaya Elektron. (Moscow) 2, 1325 (1975) [Sov. J. Quantum Electron. 5, 722 (1975)].
[5]T. P. Belikova, E. A. Sviridenkov, and A. F. Suchkov, Usp. Fiz. Nauk 113, 327 (1974) [Sov. Phys. Usp. 17, 441 (1974)].
[6]V. M. Baev, É. A. Sviridenkov, and M. P. Frolov, Kvantovaya Elektron. (Moscow) 1, 1245 (1974) [Sov. J. Quantum Electron. 4, 687 (1974)].
[7]V. M. Baev, V. L. Gulov, É. A. Sviridenkov, and M. P. Frolov, Kvantovaya Elektron. (Moscow) 2, 1328 (1975) [Sov. J. Quantum Electron. 5, 724 (1975)].
[8]É. A. Sviridenkov and M. P. Frolov, Kratk. Soobshch. Fiz. No. 3, 8 (1976).
[9]T. P. Belikova, É. A. Sviridenkov, and A. F. Suchkov, Kvantovaya Elektron. (Moscow) 1, 830 (1974) [Sov. J. Quantum Electron. 4, 454 (1974)].
[10]A. F. Suchkov, Kratk. Soobshch. Fiz. No. 1, 39 (1972).
[11]V. M. Baev, V. Vernke, and É. A. Sviridenkov, Kvantovaya Elektron. (Moscow) 2, 856 (1975) [Sov. J. Quantum Electron. 5, 477 (1975)].
[12]T. P. Belikova, É. A. Sviridenkov, and L. V. Titova, Kratk. Soobshch. Fiz. No. 5, 48 (1972).
[13]T. P. Belikova, É. A. Sviridenkov, and A. F. Suchkov, Opt. Spektrosk. 37, 654 (1974) [Opt. Spectrosc. (USSR) 37, 372 (1976)].
[14]E. N. Antonov, V. G. Koloshnikov, and V. R. Mironenko, Kvantovaya Elektron. (Moscow) 2, 171 (1975) [Sov. J. Quantum Electron. 5, 1051 (1975)].
[15]R. A. Keller, J. D. Simmons, and D. A. Jennings, J. Opt. Soc. Am. 63, 1552 (1973).
[16]T. W. Hansch, A. L. Schawlov, and P. E. Toschek, IEEE J. Quantum Electron. QE-8, 10 802 (1972).
[17]B. I. Stepanov, A. N. Rubinov, and M. V. Belokon', Zh. Prikl. Spektrosk. 24, 423 (1976).
[18]M. V. Belokon' and A. N. Rubinov, Zh. Prikl. Spektrosk. 19, 1017 (1973).
[19]C. V. Shank and M. B. Klein, Appl. Phys. Lett. 23, 156 (1973).
[20]A. P. Godlevskii, V. P. Lopasov, and S. F. Luk'yanenko, Kvantovaya Elektron. (Moscow) 2, 701 (1975) [Sov. J. Quantum Electron. 5, 388 (1975)].
[21]C. L. Tang, H. Statz, and G. de Mars, J. Appl. Phys. 34, 2289 (1963).
[22]Ch. K. Mukhtarov, Opt. Spektrosk. 21, 394 (1966) [Opt. Spectrosc. (USSR) 21, 720 (1966)].
[23]J. A. Curcio, L. E. Drummeter, and G. L. Knestrick, Appl. Opt. 3, 1401 (1964).
[24]C. E. Morre, M. G. J. Minnaert, and J. Houtgast, The Solar Spectrum from 2935 Å to 8770 Å, National Bureau of Standards, 1966.
[25]A. Chutjian and T. C. James, J. Chem. Phys. 51, 1242 (1969).
[26]R. A. Gangi and L. Burnelle, J. Chem. Phys. 55, 851 (1971).
[27]R. W. Beese, J. H. Miller, and C. J. Jun, J. Quant. Spectrosc. Radiat. Transfer 6, 717 (1966).

Translated by S. Chomet

Selective-laser-excitation study of the structure of inhomogeneously broadened spectra of Nd^{3+} ions in glass

O. K. Alimov, T. T. Basiev, Yu. K. Voron'ko, Yu. V. Gribkov, A. Ya. Karasik, V. V. Osiko, A. M. Prokhorov, and I. A. Shcherbakov

P. N. Lebedev Physical Institute, Academy of Sciences of the USSR

(Submitted 24 May 1977)
Zh. Eksp. Teor. Fiz. 74, 57–66 (January 1978)

The selective-laser-excitation technique was used to examine the structure of the inhomogeneously broadened bands of the Nd^{3+} ion in silicate glass. A survey diagram of the Stark splittings of the $^4I_{9/2}$ level in various optical centers in the glass is presented for the first time. The luminescence decay kinetics and the radiative transition probabilities A for various centers in neodymium glass are investigated. It is shown that the variations of the mean lifetime of the $^4F_{3/2}$ level under selective excitation of various optical centers in the glass correlate with the variations of A for the centers.

PACS numbers: 61.40.Df, 71.70.Ej, 78.55.Hx

Lasers with fixed wavelength, but especially tunable lasers, have recently been finding wider and wider application as excitation sources for spectroscopic studies. This is due to their unique capability of concentrating luminous energy in space, in time, and in spectrum. The use of laser sources to excite luminescence together with stroboscopic photorecorders that allow one to fix the emission (record the spectrum) instantaneously at selected times after the excitation enable one to approach the study of the Stark structure of inhomogeneously broadened spectra and the relaxation processes hidden by the inhomogeneous broadening at a qualitatively new level.[1,2]

Inhomogeneous broadening of spectra is a manifestation of the disorder of the structure of the activated

